International Conference on Space Optics—ICSO 2022

Dubrovnik, Croatia

3–7 October 2022

Edited by Kyriaki Minoglou, Nikos Karafolas, and Bruno Cugny,

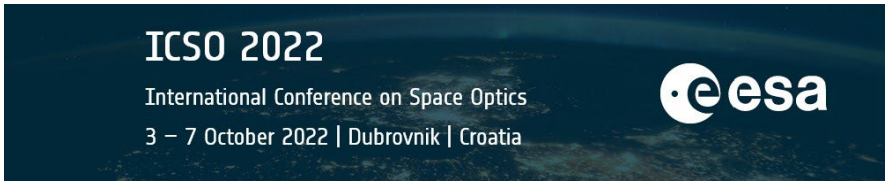

Using observational data of double stars to assess the feasibility of tip-tilt retrieval on the downlink signal for uplink pre-compensation in free space optical communications.

International Conference on Space Optics — ICSO 2022, edited by Kyriaki Minoglou, Nikos Karafolas, Bruno Cugny, Proc. of SPIE Vol. 12777, 127774E · © 2023 ESA and CNES · 0277-786X · doi: 10.1117/12.2690830

Using observational data of double stars to assess the feasibility of tip-tilt retrieval on the downlink signal for uplink pre-compensation in free space optical communications.

Monique Cockram[a], Noelia Martinez Rey[a], Adelaide Gilling , and David Alaluf[b]

[a]Australian National University, Research School of Astronomy and Astrophysics, Mount Stromlo Observatory, Cotter Road, Weston Creek 2611, Australia
[b]European Space Research and Technology Centre, European Space Agency, Noordwijk, The Netherlands

ABSTRACT

Free space optical communications with satellites are affected by atmospheric turbulence, typically using adaptive optics to correct for the resulting signal errors. This can be done using laser guide stars as a reference signal for the wavefront sensing, with the exception of tip-tilt, which up to date cannot be reliably measured with laser guide stars. Proposed solutions utilise the downlink signal (sent from satellite to ground station) as a reference source with which to pre-compensate for tip-tilt in the uplink signal. However, the point ahead angle due to the orbital motion of the satellites results in the signals propagating through different regions of the atmosphere. Due to atmospheric anisoplanatism, there is a degree of tip-tilt decorrelation between the laser links. The purpose of this study is to determine if the tip-tilt is sufficiently correlated such that the downlink can still be used as a reference source for adaptive optics applied to the uplink signal. This project developed methods to measure the tip-tilt of double stars and analyse the correlation of these effects between the two component stars, equivalent to the downlink and uplink signals. Observational data of double stars at Mount Stromlo Observatory (Canberra, Australia) at different elevations and separations are analysed to obtain statistics of the differential atmospheric tip-tilt in strong turbulence regimes in the Southern Hemisphere; results are compared with similar studies carried out in the Northern Hemisphere. This work aims to assess the feasibility of using the downlink as a reference signal for atmospheric tip tilt sensing with the goal of improving the performance in the uplink communications.

Keywords: FSO communications, uplink correction, adaptive optics, tip-tilt

1. INTRODUCTION

Free space optical communications experience signal loss and overall decrease in performance due to the turbulence in the atmosphere. Adaptive optics can be used to correct for the majority of these aberrations using a reference light source on the sky. Due to the point ahead angle between uplink and downlink in bidirectional optical communications, the satellite signal might not be adequate to act as this reference source. Laser guide stars can overcome this challenge. However, the tip-tilt indetermination problem is yet to be solved.

1.1 Free Space Optical Communications

As improvements to satellite communication continue, the benefits of expanding from radio frequencies to optical signals become more important. Free space optical (FSO) communications with satellites transmit line-of-sight signals using modulated laser beams between different types of links; ground station to satellite, satellite to ground station, and horizontal links between ground station and ground station, or between satellite and satellite.

Using optical lasers for FSO communications has a much higher data rate than when using radio frequencies,[1] making it more feasible to transfer the large quantities of data that are becoming more and more prevalent. Additionally, there are less power requirements for optical laser links, since the beam spread is narrower than

Further author information: (Send correspondence to Noelia Martinez Rey: E-mail: noelia.martinezrey@anu.edu.au

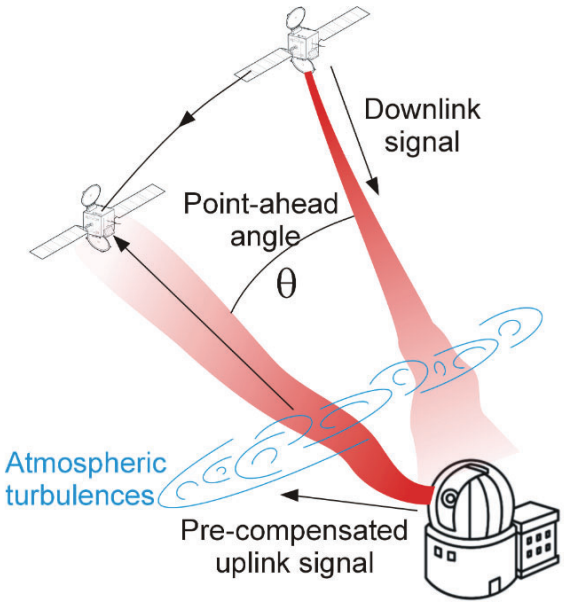

Figure 1: The point ahead angle of the uplink signal with respect to the downlink signal. The two signals must travel through different regions of atmospheric turbulence.[6]

that of radio frequencies.[2] This also results in higher security data transmission, as there is inconsiderable interception of the line-of-sight laser signals.[3] Currently, there are less regulations and restrictions on frequencies due to high demand than with radio signals. Therefore, interference with other links is reduced.

However, the use of optical wavelengths for satellite communication has specific challenges of signal distortion due to atmospheric turbulence which does not affect radio signals. These are a significant source of error, and are discussed further in Section 1.1.1. Another practical element of signal transmission is that any jittering of the transmitter or receiver due to environmental interference contributes to the degradation of the signal.[4]

Due to the orbital motion of these satellites, the uplink (ground station to satellite) and downlink (satellite to ground station) signals are spatially separated by the point-ahead angle, shown in Figure 1. This angle is defined by $2v/c$,[5] where c is the speed of light and v is the orbital velocity of the satellite. The point-ahead angle of a geostationary satellite is approximately 4 arcseconds, and that of a satellite in low Earth orbit is dependent on the orbital radius, however with the example of the International Space Station (ISS), has an angle of around 10 arcseconds.[6] The point-ahead angle results in the uplink and downlink laser beams to propagate through different regions of the atmosphere, and thus experience different atmospheric turbulence effects, as discussed further in Section 1.1.2.

1.1.1 Atmospheric Turbulence Effects

Turbulence in the atmosphere is caused by fluctuations in temperature and pressure across different regions of the atmosphere. These result in random inhomogeneities in the refractive index of the atmosphere along the transmission path of light, distorting the intensity and phase of the signal wavefront being sent between satellite and ground station.[7] In turn, this contributes significantly to the noise in the received signal and increases the bit error rate (BER).

The impact of atmospheric turbulence on laser beams for satellite optical communications can be broadly categorised into the effects of beam wander, beam spreading, and scintillation.[8] Beam wander is caused by lower order atmospheric turbulence effects, and is observed as a variance in displacement of the beam on the detector.[9] This is also referred to as tip-tilt, and is discussed further in Section 1.1.2.

For satellite communications, the turbulence affects the uplink and downlink signals differently. The turbulence differences between propagation directions need to be added to the differences due to the point-ahead

angle.[10] Turbulence eddy currents are of different sizes and cause different effects throughout the layers of the atmosphere. The uplink beam is generated on the ground, where the size of the laser beam is on the same order of magnitude as the turbulence eddy currents. However, since the downlink beam originates in space, beam spreading causes it to be on a much larger scale than the turbulence. Therefore, the turbulence effects on the uplink and downlink signals are different. For example, the effects of beam spreading primarily occurs in turbulence nearer to ground-based transmitters. As a result, the beam radius of uplink signals at the detector is larger than that of the downlink signals.[11]

1.1.2 Tip-Tilt and the Isokinetic Angle

The first order aberration of tip-tilt causes the direction of propagation of the light beam to deviate. These changes to the angle of the incoming signal offset the location of an image on the observation screen or detector. This causes the previously described beam wandering effect, which can result in the signal moving around on the detector, or even missing it entirely. It is important to correct for such aberrations in order to minimise the BER by ensuring the signal is always reaching the detector, without having to use detectors with unrealistically large fields of view. Since tip-tilt aberrations cause the movement of a signal around the area of the detector, the magnitude of tip-tilt can be expressed as the variance in the detected beam location.

Regions of the atmosphere that have the same atmospheric turbulence effects on light are called isoplanatic. Within an isoplanatic angle, the aberrations on different light beams are considered to be correlated. The tip-tilt isoplanatic region, or the isokinetic region, is where the tip-tilt effects on light are correlated.[12]

The isokinetic angle varies across the atmosphere due to factors like temperature and different air pressure systems, all of which are characterised by the refractive index structure constant, C_n^2. Additionally, the elevation of a beam also impacts the isokinetic angle. Transmission closer to the horizon results in higher turbulence effects due to longer propagation through denser layers of the atmosphere. As a result, the elevation of sources is of interest when detecting signals. The elevation is also important when applying the point ahead angle required for satellite communications, since the laser links are each travelling through different areas of the atmosphere which could each have different characteristics of turbulence. If the point-ahead angle is larger than the isokinetic angle, the laser links will acquire different tip-tilt effects.[5]

A focus on correcting for tip-tilt emerges from the fact that lower order modes have the highest contribution to the total wavefront error, around 85%.[6] Additionally, the isokinetic angle is typically larger than that of the higher order aberrations.[5] Hence, there is a higher possibility that the point-ahead angle is within the isokinetic angle, increasing the likelihood that the signals experience correlated tip-tilt effects.

Adaptive optics (AO) can be applied to satellite optical communications to minimise the errors due to atmospheric turbulence, like tip-tilt.[5] The light propagation of a laser guide star (LGS) through the atmosphere in both directions (up into the atmosphere and then returning to ground) results in the tip-tilt effect to be cancelled out once it reaches the ground based detector.[13] As a result, conventional AO using LGSs cannot be used to correct wavefront slope effects due to tip-tilt. Instead, natural guide stars must be used, which are natural stars of known constant flux that are used as a reference source for AO. In order to correct for this tip-tilt effect in satellite communications where there are no natural guide stars available, this project proposes that the downlink signal could be used as a reference source to correct for these atmospheric low order modes in the uplink signal. This research follows from the work of Alaluf et al. (2021),[6] with the purpose of undertaking a similar study in the southern hemisphere. In order to assess the feasibility of this process, correlated tip-tilt effects need to be confirmed to determine if the two laser beams are traveling through the same isokinetic area.[5] Such correlation would enable the turbulence in downlink signals to be used to characterise the pre-compensation needed to be applied to uplink signals to minimise BER.

For this project, double stars with different separation angles were used to determine if the uplink and downlink signals could be in the same isokinetic region. Double stars consist of two stars close together from the perspective of Earth-based observations, hence making them an appropriate analogue for the bidirectional signals from satellites, as shown in Figure 2. The separation between the components of double stars mimics the different orbital radii of bidirectional communications satellites; the closer the components of the double stars, the larger the orbital radius of the satellite.

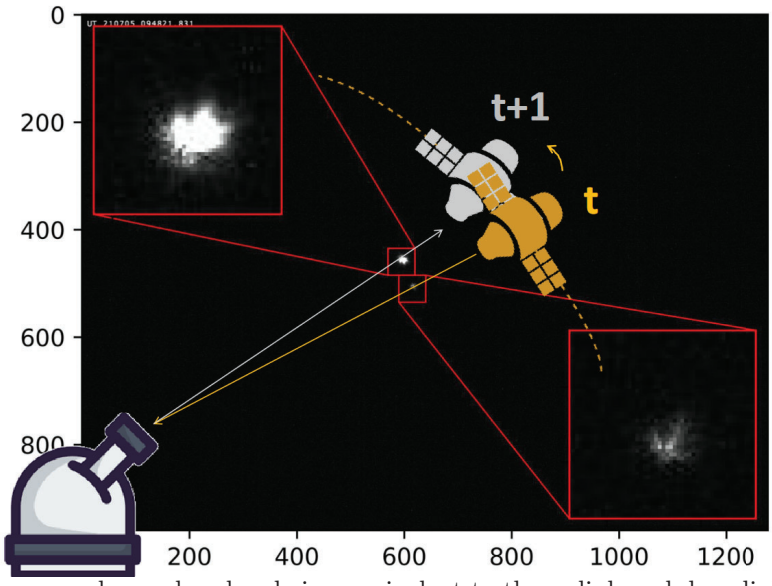

Figure 2: Double stars are can be analysed as being equivalent to the uplink and downlink signals of satellite to ground station free space optical communications.

The methodology in Section 2 outlines the data processing methods written in `Python` code to calculate the tip-tilt of any double star data sets. These methods enabled the analysis of the atmospheric tip-tilt effects to determine the correlation between the two light sources.

2. METHODS

The data used in this research consists of observations of double stars at different elevations. The separation between each star in the pair was chosen to be representative of various point-ahead angles. Each component star was analysed independently to compare the tip-tilt of two separated signals. The data set is outlined in Appendix A.

2.1 Removal of Background Noise

Background noise and isolation of each of the stars are performed prior to the testing of several centroiding methods as described in Section 2.2. Due to the difference in magnitudes between the primary and secondary stars, each one was isolated and processed separately. Figure 3 shows an example where the reader can see the clear difference in magnitude between the two selected stars.

Firstly, a binary image of the star was created based on a chosen threshold, to use as a mask. This binary mask was then multiplied by the original in order to produce a background-noise removed image where only relevant star pixels have values greater than zero, an example of which is shown in Figure 4(b). The centre of each star was found to be more accurate by following this procedure.

An appropriate threshold value was characterised as being large enough to remove any low valued background noise pixels that don't contribute to the structure of the star being observed, as in the comparison between Figures 4(a) and 4(b). Additionally, the threshold must not be too large to result in the discarding of dimmer yet still important features of the star. Figure 4(c) demonstrates how an incorrect choice of threshold value will cut off the outer pixels of the star.

In order to select the most appropriate threshold value for each star, verification tests were performed to quantify the extent to which threshold values affect the calculated centre for a given star. A range of threshold values were implemented and the resulting centres were obtained and examined by eye. Additionally, the average change in centre of each star over all the frames of data was determined. This enabled the comparison of change of the centroid values between frames to that of the change of centroid values due to variations in the chosen

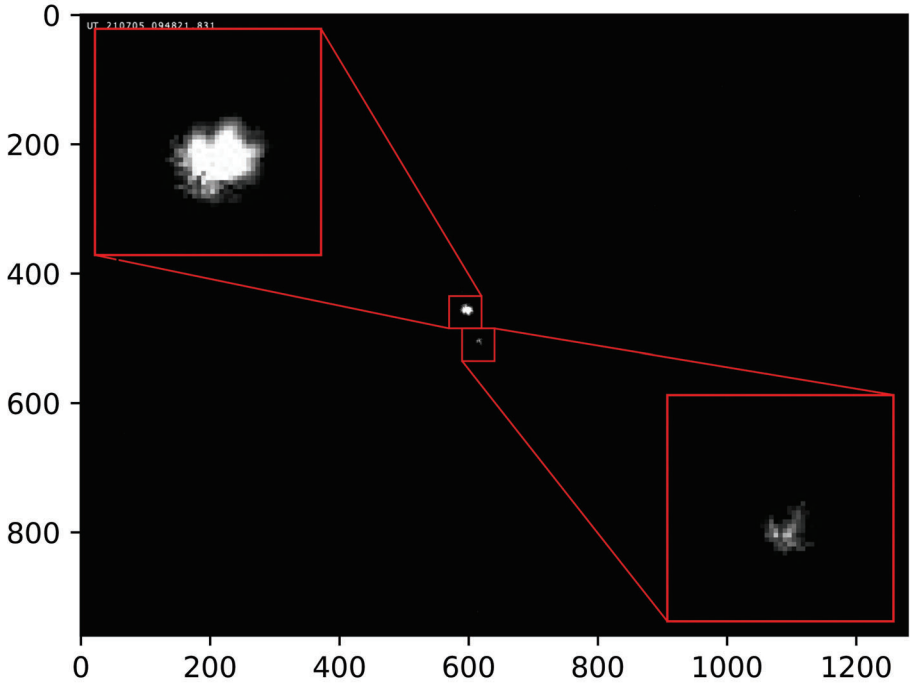

Figure 3: Isolating the primary and secondary stars so that binary masks with different threshold values can be applied to each one separately.

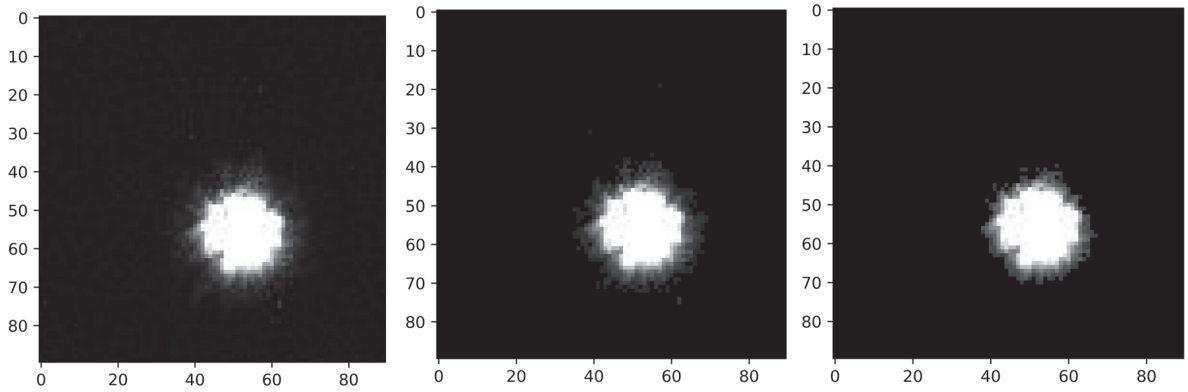

(a) Threshold value set to zero, no background noise has been removed.

(b) Threshold value appropriate.

(c) Threshold value set too high.

Figure 4: The effect of threshold values on the background-removed images. The primary star of H 3 7 used as an example.

threshold value. If the size of the changes between frames were found to be much larger than the order of the changes due to thresholding, then less care would need to be taken than if the converse were true.

To determine the effect that the threshold value has on the tip-tilt analysis, the centroid of each star was found through the range of threshold values. Across the range of threshold values, the standard deviation of the star's distance from the origin was recorded. This was done for both the primary and secondary stars. The range of threshold values where the output of the analysis was stable was used to guide the appropriate choice. Threshold values were chosen to be in this region to ensure consistent results, where small differences in chosen threshold value do not significantly impact the centroiding algorithm.

The stable regions were compared with the observations by eye to determine the most appropriate threshold value to use when creating the binary mask.

2.2 Centroiding

Various methods for calculating the location of a star in an image were tested to determine the most accurate method for these data sets. A centre of mass method for finding the centre of the primary and secondary stars was determines to be the most appropriate for this application. This method involved using the different intensities of each pixel to find a centre of mass of the light detected from the star. In this way, the contribution of each pixel to the centre of the star was weighted by its intensity value, as expressed in Equation 1, where the pixels x_j were weighted by their intensities I_j.

$$CoM = \frac{\sum_j (x_j \times I_j)}{\sum_j I_j} \tag{1}$$

2.3 Tip-Tilt Analysis

To analyse the tip-tilt of the wavefront, two types of movement of the double stars were analysed; relative and absolute. These two analysis methods both made use of the centroids of the primary and secondary stars found for each frame of data using methods in Section 2.2.

2.3.1 Differential Tip-Tilt

First, the distance between the two stars was recorded for each frame. If the two stars were within the isokinetic angle of the atmosphere, they would maintain the same relative position. Therefore, the amount of variation in the separation of the stars was relative to the decoherence of tip-tilt due to different atmospheric effects. The differential tip-tilt was expressed as the standard deviation of the distances between the two stars across the frames of data.

2.3.2 Tip-Tilt Correlation

Second, the motion of the centroid of each star relative to its position in the first frame of data was recorded. The difference between these motions of the two stars was used to determine the correlation of tip-tilt motion. The horizontal and vertical motions of each star were recorded separately, so as to maintain both the direction and magnitude of the motion. To quantify the coherence of the tip-tilt aberration on the two objects in the double star, a correlation coefficient matrix was generated. Only two elements of this matrix are relevant; the correlation between the horizontal movements of both the primary and secondary stars, and that of the vertical movements. In an ideal scenario, double stars that are in the same isokinetic region will have correlation coefficients equal to 1.

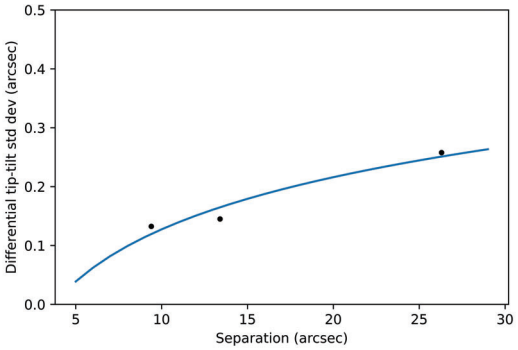

(a) Differential tip-tilt results with fitted curve (respectively in black dots and blue filled line).

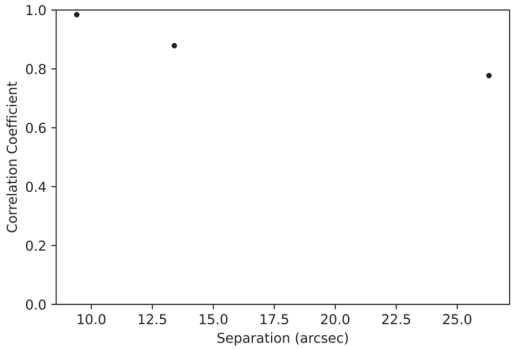

(b) Correlation coefficients.

Figure 5: Differential tip-tilt and correlation coefficients for double stars of different separations, observed at approximately 80° from the horizon. Blue line corresponds to the Modified Hufnagel-Valley Model prediction.

3. RESULTS

3.1 Tip-tilt Analysis

The standard deviations of the differential tip-tilt across all the frames of data was found for each double star, to observe how the apparent distance between the stars shift due to the tip-tilt aberrations. Additionally, for each double star a correlation matrix was used to determine if the tip-tilt of the primary and secondary stars was correlated. Tip-tilt effects that are exactly equal have a correlation value of 1, and that of uncorrelated stars is 0. This demonstrates the effects of elevation and separation of the two sources of light in determining how correlated the tip-tilt aberrations are

Figure 5(a) demonstrates the relationship of the standard deviation of the differential tip-tilt to the separation of the double stars. As the separation between the two stars increases, so does the differential tip-tilt, due to the larger difference in atmosphere that each signal was travelling through. This is similarly demonstrated in Figure 5(b), where the correlation of measured tip-tilt between stars is at its highest when the stars are closest together. These results confirm that smaller correlation coefficients of the tip-tilt effects of each star are observed as their separation approaches or exceeds the isokinetic angle.

Additionally, a single double star, DUN 126, was observed at three different elevations, as shown in Figure 6. This enabled an investigation into the effect of the elevation from the horizon of a signal's path through the atmosphere. Figure 6(a) demonstrates a decrease in differential tip-tilt as the stars are observed closer to zenith. This is supported by the correlation coefficient data in Figure 6(b). Due to the fact that the isokinetic angle is also smaller for observations made with telescope elevations closer to the horizon, the tip-tilt was more highly decorrelated for angles further from zenith.

In comparison to the work of Alaluf et al.,[6] a similar relationship between differential tip-tilt and both elevation and separation was obtained. The Modified Hufnagel-Valley Model was used to predict the expected differential tip-tilt at Mount Stromlo Observatory; the fitted curves in Figures 5(a) and 6(a) present these results, showing a stronger decorrelation of tip-tilt for a change in elevation, than that due to an increase in separation of the signals. Further expansion of the data set used in this paper should continue to verify these results and the comparison. Overall, for observations closer to the horizon, larger deviation in tip-tilt was observed as the light has to travel through thicker atmosphere. Larger separations between the two components of the double stars have the same effect, due to the difference in atmosphere that the two light sources propagate through.

3.2 Measurement of Seeing

Seeing is not known exactly at Mount Stromlo Observatory (MSO) where the observational data was taken, as the atmosphere has not been characterised. The seeing can be estimated using the point spread functions (PSFs)

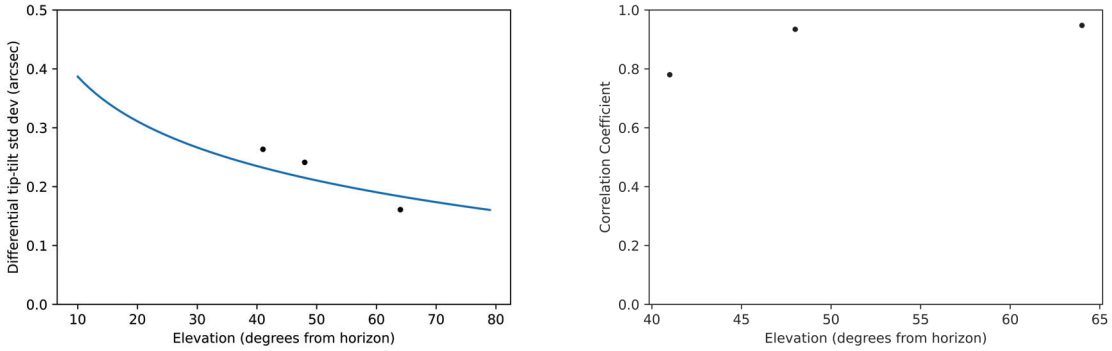

(a) Differential tip-tilt results with fitted curve (respectively in black dots and blue filled line).

(b) Correlation coefficients.

Figure 6: Differential tip-tilt and correlation coefficients for the same double star, DUN 126, observed at different elevations from the horizon. Blue line corresponds to the Modified Hufnagel-Valley Model prediction.

Table 1: Approximated seeing values for two nights of observation found from data of double stars.

Double Star	Seeing (″)	
	13 June 2022	24 July 2022
DUN 126	2.83	2.03
DUN 42	1.86	1.66

of observed stars. The full width at half maximum (FWHM) of these PSF is inversely proportional to the Fried's parameter r_0, and thus an expression of the seeing.[14] By fitting a Gaussian curve to the cross section of the star, the PSF can be approximated. The FWHM of this fitted Gaussian is $2\sqrt{2\ln 2}\sigma$.

The PSF of the double stars outlined in Appendix A were computed for both stars in each frame, and the average FWHM of all PSFs were recorded. It was clear that the seeing declined at telescope elevations closer to the horizon, which was expected.

Since seeing is conventionally defined at zenith, an overall value for seeing at the MSO site was found by using trigonometry to convert the FWHM values to that of seeing at zenith. The following equation was used:

$$\varepsilon_0 = \sigma_{FWHM} \cos\alpha \tag{2}$$

where ε_0 is the seeing, σ_{FWHM} is the FWHM of the PSF, and α is the observed angle of the star from zenith.

Applying Equation 2 gives the results in Table 1.

Combining the results from Table 1, the seeing at MSO was experimentally estimated to be 2″.

Additionally, this estimation of seeing enabled an estimation of the Fried parameter using Equation 3. An experimentally estimated Fried parameter of 5cm at 550nm was obtained.

$$\varepsilon_0 = \frac{0.976\lambda}{r_0} \tag{3}$$

4. DISCUSSION

The observational data of double stars enabled a preliminary investigation into the effects of elevation and separation on the correlation between two signals. Whilst these data sets show very useful and promising results, there is a need to continue increasing the data set in order to obtain clear statistics on the tip-tilt measurements across the sky and at times of different seeing conditions.

4.1 Uplink Tip-Tilt Correction

Applying the developed methodology to a range of double stars enables an overview of the way in which atmospheric tip-tilt changes across the atmosphere. By comparing the results of tip-tilt determination across double stars of different separations, the decrease in coherence between the two stars was clear, as in Section 3.1. Where two signals have greater spatial separation, the further they are from being within the isokinetic angle, resulting in low correlation between the tip-tilt effects that each of the signals exhibit. Additionally, the different elevations of observations of the same double star result in signals travelling through different regions and thicknesses of the atmosphere. It follows from the dependence of $C_n^2(h)$ on height and the intuitive sense of propagation at lower elevations meaning propagation through larger distance of atmosphere, that the isokinetic angle also decreases closer to the horizon, and that the tip-tilt correlation was the lowest towards this end of the range. Despite these atmospheric effects, the values in Figures 5(b) and 6(b) demonstrate high levels of correlation of the observed tip-tilt between the primary and secondary stars of the three double stars. This suggests promising potential for feasibility in using the downlink signal as a reference to correct for tip-tilt in the uplink signal.

The results can be verified with the work of Alaluf et al.,[6] in which similar data was taken in the northern hemisphere. The fitted curves of the observational data in this paper show a clear comparison of the differential tip-tilt measured and simulated by Alaluf et al. This verification of results will be expanded on as more observational data is obtained.

The elevation of the double stars is clearly analogous to the position of satellites in the sky, and differences in the separation of the stars are comparable to the point ahead angle between downlink and uplink signals due to the orbital motion of satellites. As such, the comparison of the results of the double stars in this project to the FSO satellite communications applications is clear.

Signals with separations as large as $26.3''$ show correlation values of tip-tilt larger than 0.75. Further observational data sets are needed to verify these preliminary findings. The results suggest a possibility that the downlink signal has tip-tilt effects similar enough to the uplink signal such that it can be used as a reference source for tip-tilt sensing in adaptive optics.

5. CONCLUSION

The relationships between tip-tilt and the separation and elevation of observed double stars were investigated to gain an understanding of their behaviour. It was measured that signals propagating closer to the horizon have more significant differences in tip-tilt, and as a result a smaller isokinetic angle. Additionally, signals had more highly correlated tip-tilt the closer together their propagation paths were. In both investigations, highly correlated tip-tilt effects were observed, even those with less desirable elevations or separations.

The results show reasonable correlation coefficients of tip-tilt between the primary and secondary stars of the observational data, demonstrating that signals could be within the isokinetic angle. More extensive observations would allow for more robust statistics to use in an assessment of the feasibility of FSO communications using the downlink signal as a reference source to pre-compensate for the tip-tilt in the uplink signal.

Data is being regularly taken to increase the data sets and further verify these preliminary results. Data sets are available upon request. Future data sets will include daytime observations, to further characterise the feasibility of this uplink tip-tilt correction.

APPENDIX A. DATA SET

Various data sets of nighttime observations of double stars were used for analysis in this research. They consisted of 2min videos, over a range of integration times per frame of 1ms, 5ms, and 10ms. The longer integration time means that the tip-tilt effects become averaged as they are recorded, rather than obtaining a snapshot of the atmosphere. The shorter integration times were used for analysing the effects of tip-tilt over a period of time using multiple consecutive frames of data.

The double star images were selected from observation runs taken on the nights of 21 July 2021, 13 June 2022, and 24 July 2022 using the McNamara-Saunders Astronomical Teaching Telescope 1 (MSATT1) located on the Mount Stromlo Observatory (MSO), Canberra, Australia. The double stars were chosen based on the following criteria:

- The separation between primary and secondary stars needs to be large enough to be resolved (estimated at greater than 5").
- The double stars need to have sufficient brightness to be easily observable (at a magnitude of approximately 4 or brighter).
- The same double star (or different double stars of approximately the same separation) needs to be imaged over a range of different elevations
- Double stars of different separations need to be observed at approximately the same telescope elevation.

The time and weather constraints of the observation runs also determined which double stars were able to be imaged. Double stars of different separations and imaged at different telescope elevations were chosen, and are outlined in the tables below. Additional double stars were observed in other ranges of separation or elevation, however only one group of each was discussed in this research. The observations resulted in videos of frame length equal to the integration time. Each frame is an image that was analysed separately.

The specifications of the MSATT1 telescope used to collect the double star observational data are outlined in Table 4.

Table 2: Double star observed at elevation approximately 80°.

Double Star	Elevation (°)	Separation (″)	Observation Date
H 3 96	84	9.4	13 June 2022
DUN 177	75	26.3	24 July 2022
H 3 7	73	13.4	24 July 2022

Table 3: Double star DUN 126, separation 34.5″, observed at different elevations across three nights of observation.

DUN 126	Elevation (°)	Observation Date
	41	21 July 2021
	64	13 June 2022
	60	24 July 2022

ACKNOWLEDGMENTS

The authors would like to thank Geoffrey McNamara, manager of McNamara-Saunders Astronomical Teaching Telescope (MSATT) and the Science Mentors ACT program, for his support to the project. The authors would also like to acknowledge the very productive discussions with Professor Celine d'Orgeville and colleagues at the Advanced Instrumentation and Technology Centre, and with Dr James Osborn from Durham University.

Table 4: MSATT1 telescope specifications.

Feature	Specification
Camera	ZWO ASI120MM-S
Detector	CMOS AR0130CS
Field of View (arcmin)	5.6×4.2
Detector size (pixels)	1280×960
Plate scale (arcsec/pixel)	0.2625
Aperture (mm)	300

REFERENCES

[1] Koishi, Y., Suzuki, Y., Takahashi, T., Mase, I., Jibiki, M., Hashimoto, Y., Murata, S., Yamashita, T., and Shiratama, K., "Research and development of 40gbps optical free space communication from satellite/airplane," in [*2011 International Conference on Space Optical Systems and Applications (ICSOS)*], 88–92, IEEE (2011).

[2] Kaushal, H. and Kaddoum, G., "Optical communication in space: Challenges and mitigation techniques," *IEEE communications surveys & tutorials* **19**(1), 57–96 (2016).

[3] Chaudhary, S. and Amphawan, A., "The role and challenges of free-space optical systems," *Journal of Optical Communications* **35**(4), 327–334 (2014).

[4] Polishuk, A. and Arnon, S., "Optimization of a laser satellite communication system with an optical preamplifier," *JOSA A* **21**(7), 1307–1315 (2004).

[5] Martínez, N., Rodríguez-Ramos, L. F., and Sodnik, Z., "Toward the uplink correction: application of adaptive optics techniques on free-space optical communications through the atmosphere," *Optical Engineering* **57**(7), 076106 (2018).

[6] Alaluf, D. and Armengol, J., "Ground-to-satellite optical links: how effective is an uplink tip/tilt precompensation based on the satellite signal?," *CEAS Space Journal* , 1–12 (2021).

[7] Wyngaard, J. C., "Atmospheric turbulence," *Annual Review of Fluid Mechanics* **24**(1), 205–234 (1992).

[8] Davis, J., "Consideration of atmospheric turbulence in laser systems design," *Applied Optics* **5**(1), 139–147 (1966).

[9] Mahdieh, M. and Pournoury, M., "Atmospheric turbulence and numerical evaluation of bit error rate (ber) in free-space communication," *Optics & Laser Technology* **42**(1), 55–60 (2010).

[10] Ji, X., Chen, H., and Ji, G., "Characteristics of annular beams propagating through atmospheric turbulence along a downlink path and an uplink path," *Applied Physics B* **122**(8), 1–11 (2016).

[11] Du, W., Zhu, H., Liu, D., Yao, Z., Cai, C., Du, X., and Ai, R., "Effect of non-kolmogorov turbulence on beam spreading in satellite laser communication," *Journal of Russian Laser Research* **33**(5), 456–463 (2012).

[12] Mata-Calvo, R., Calia, D. B., Barrios, R., Centrone, M., Giggenbach, D., Lombardi, G., Becker, P., and Zayer, I., "Laser guide stars for optical free-space communications," in [*Free-Space Laser Communication and Atmospheric Propagation XXIX*], **10096**, 188–199, SPIE (2017).

[13] Davies, R. and Kasper, M., "Adaptive optics for astronomy," *Annual Review of Astronomy and Astrophysics* **50**, 305–351 (2012).

[14] Martinez, P., "Multiwavelength active-optics shack-hartmann sensor for monitoring seeing and turbulence outer scale," *Astronomy & Astrophysics* **572**, A14 (2014).